SOCIETY FOR SCIENCE AND EDUCATION
UNITED KINGDOM
TMLAI TRANSACTIONS ON MACHINE LEARNING AND ARTIFICIAL INTELLIGENCE
ISSN 2054-7390

Support Vector Machine Regression and Artificial Neural Network for Channel Estimation of LTE Downlink in High-Mobility Environments

[1*]Anis Charrada and [2]Abdelaziz Samet
[1]SERCOM Laboratory, Tunisia Polytechnic School, University of Carthage, Tunis, Tunisia;
[*]Tunisian Military Academy, Tunisia;
[2]INRS, EMT Center, 800 de la Gauchetière W., Suite 6900, Montreal, QC, H5A 1K6, CANADA;
anis.charrada@gmail.com

ABSTRACT

In this paper we apply and assess the performance of support vector machine regression (SVR) and artificial neural network (ANN) channel estimation algorithms to the reference signal structure standardized for LTE Downlink system. SVR and ANN where applied to estimate real channel environment such as vehicular A channel defined by the International Telecommunications Union (ITU) in the presence of nonlinear impulsive noise. The proposed algorithms use the information provided by the received reference symbols to estimate the total frequency response of the time variant multipath fading channel in two phases. In the first phase, each method learns to adapt to the channel variations, and in the second phase it predicts all the channel frequency responses. Finally, in order to evaluate the capabilities of the designed channel estimators, we provide performance of SVR and ANN, which is compared with traditional Least Squares (LS) and Decision Feedback (DF). The simulation results show that SVR has a better accuracy than other estimation techniques.

Keywords: Complex SVR; ANN; nonlinear impulsive noise; OFDM and LTE.

1 Introduction

The Long Term Evolution (LTE) is a step towards the fourth generation (4G) of mobile radio technologies to obtain higher throughput and to increase the spectral efficiency. Fourth-generation broadband wireless multiple access systems have data rate specifications on the order of hundreds of Mb/s. For an LTE system with 20 MHz bandwidth, the objective is for the Downlink (DL) and Uplink (UL) peak data rates to require 100 and 50 Mb/s, respectively [1].

LTE Downlink uses Orthogonal Frequency Division Multiplex Access (OFDMA) radio interface, that is support high data rate capabilities and it is more resilient against severe channel conditions. OFDMA technique essentially distributes the symbols of a large number of carriers. By implementing this new access technique in the context of mobile broadband transmission, new approaches for time and frequency equalization, synchronization and channel estimation are needed.

Because channel estimation is an important concern of LTE DL, some research results have been published, including Least Squares (LS) and Minimum Mean Square Error (MMSE)-based techniques such

DOI: 10.14738/tmlai.44.2145
Publication Date: 25th August, 2016
URL: http://dx.doi.org/10.14738/tmlai.44.2145

as [2] and [3] where the authors have studied the performance of two linear channel estimators, the Least Squares Error (LSE) and the Linear MMSE (LMMSE).

In LTE with a time variant highly selective multipath fading channel, where complicated nonlinearities can be found (the channel variations in time and in frequency domain are nonlinear in addition to the presence of impulsive noise), the accuracy of estimation can significantly decrease by applying the linear process.

ANN can perform complex mapping between its input and output space and are capable of forming complex decision regions with nonlinear decision boundaries [4]. Further, these networks of different architectures have found successful application in channel estimation problems because of their nonlinear characteristics. ANN is proposed as a channel estimator for QPSK and QAM constellation, respectively in [5] and [4].

In this paper, we designed first a Back Propagation Algorithm BPA-based ANN channel estimation technique for LTE-OFDM system over frequency selective multipath fading channel in the presence of nonlinear impulsive noise interfering with reference symbols under high mobility conditions.

In addition, we designed a complex Support Vector Machine Regression (SVR) based on Radial Basis Function (RBF) kernel for channel estimation in LTE DL that maps the input vector from a finite-dimensional space (the input space) to a higher dimensional Hilbert space (can be infinity) which it is provided with a dot product. Training SVR approach is used for channel estimation of highly selective multipath channels for OFDMA systems where the LS algorithm was applied in the training step as a channel estimator: it uses the obtained estimations as a dataset for training. The idea is to exploit the information supplied by the pilot symbols in order to estimate the channel frequency response.

The organization of this paper is as follows. In section 2, description of LTE Downlink system model is given. ANN based LTE channel estimator is introduced in section 3. In section 4, a nonlinear channel estimator based on the complex SVR is provided. Simulation results are offered in section 5. Finally, section 6 concludes the paper.

2 LTE Downlink System Model

The LTE DL system is based on the OFDMA air interface transmission scheme. Figure 1 shows the block diagram of the baseband equivalent system model.

Let us consider an LTE Downlink system which comprises N subcarriers, occupying a bandwidth *B*. The corresponding OFDM system consists firstly of mapping binary data streams into complex symbols by means of QAM modulation. Then data are transmitted in frames by means of serial-to-parallel conversion. Some pilot symbols are inserted into each data frame which is modulated to subcarriers through the Inverse Discret Fourier Transform (IDFT). These pilot symbols are inserted for channel estimation purposes. The IDFT is used to transform the data sequence $X(k)$ into time domain signal.

One guard interval (GI) is inserted between every two OFDM symbols in order to eliminate Inter-Symbol Interference (ISI). This guard time includes the cyclically extended part of the OFDM symbol in order to preserve orthogonality and eliminate Inter-Carrier Interference (ICI). It is well known that if the channel impulse response has a maximum of L resolvable paths, then the GI must be at least equal to L [6]. Thus, each OFDM symbol is transmitted in time T and includes a cyclic prefix of duration T_{cp}. Therefore, the duration of each OFDM symbol is $T_u = T - T_{cp}$. Every two adjacent subcarriers are spaced by $\delta f = 1/T_u$. The output signal of the OFDM system is converted into serial signal by parallel to serial converter. A

complex Additive White Gaussian Noise (AWGN) process $N\left(0,\sigma_{w_g}^2\right)$ with power spectral density $N_0/2$ is added through a frequency selective time varying multipath fading channel.

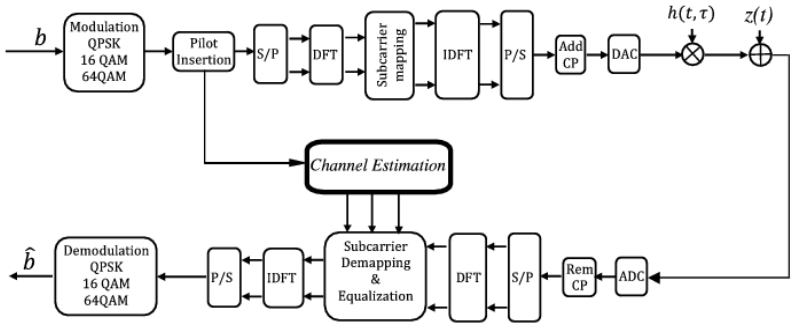

Figure 1: Block diagram of the baseband equivalent system model.

In a practical environment, impulsive noise can be present, and then the channel becomes nonlinear with non Gaussian impulsive noise. The impulsive noise can significantly influence the performance of the OFDM communication system for many reasons. First, the time of the arrival of an impulse is unpredictable and shapes of the impulses are unknown and they vary considerably. Moreover, impulses usually have very high amplitude, and thus high energy, which can be much greater than the energy of the useful signal [7].

The impulsive noise is modeled as a Bernoulli-Gaussian process and it was generated with the Bernoulli-Gaussian process function $i(n) = v(n)\,\lambda(n)$ where $v(n)$ is a random process with Gaussian distribution and power σ_{BG}^2, and $\lambda(n)$ is a random process with probability [8]

$$P_r(\lambda(n)) = \begin{cases} p & \lambda = 1 \\ 1-p, & \lambda = 0. \end{cases} \tag{1}$$

At the receiver side, and after removing guard time, the discrete-time baseband OFDM signal can be expressed as

$$y(n) = \sum_{k\in\{\Omega_P\}} X^P(k)H(k)e^{j\frac{2\pi}{N}kn} + \sum_{k\notin\{\Omega_P\}} X^D(k)H(k)e^{j\frac{2\pi}{N}kn} + w_g(n) + i(n) \tag{2}$$

where Ω_P the subset of N_P pilot subcarriers, $X^P(k)$ and $X^D(k)$ are complex pilot and data symbol respectively, transmitted at the k^{th} frequency and $H(k) = DFT_N\{h(n)\}$ is the channel's frequency response at the k^{th} subcarrier. Note that, pilot insertion in the subcarriers of every OFDM symbol must satisfy the demand of the sampling theory and uniform distribution [9].

Assuming that ISI are eliminated after DFT transformation, therefore $y(n)$ becomes

$$Y(k) = X(k)H(k) + W_G(k) + I(k) = X(k)H(k) + e(k), \quad k = 0,\cdots,N-1 \tag{3}$$

where $e(k)$ is the residual noise which represents the sum of the AWGN noise $W_G(k)$ and impulsive noise $I(k)$ in the frequency domain, respectively.

Equation (3) may be presented in matrix notation as follows:

$$Y = \boldsymbol{X}\boldsymbol{F}h + W + I = \boldsymbol{X}H + e \tag{4}$$

where

$$\boldsymbol{X} = diag\big(X(0), X(1), \cdots, X(N-1)\big)$$

$$Y = [Y(0), \cdots, Y(N-1)]^T$$

$$W_G = [W_G(0), \cdots, W_G(N-1)]^T$$

$$I = [I(0), \cdots, I(N-1)]^T$$

$$H = [H(0), \cdots, H(N-1)]^T$$

$$e = [e(0), \cdots, e(N-1)]^T$$

$$\boldsymbol{F} = \begin{bmatrix} F_N^{00} & \cdots & F_N^{0(N-1)} \\ \vdots & \ddots & \vdots \\ F_N^{(N-1)0} & \cdots & F_N^{(N-1)(N-1)} \end{bmatrix}$$

and $$F_N^{i,k} = \left(\frac{1}{\sqrt{N}}\right) exp^{-j2\pi\left(\frac{ik}{N}\right)}. \quad (5)$$

3 ANN Estimation

Artificial Neural Networks (ANN) are one of the widespread branches of artificial intelligence. They have very simple neuron-like processing elements (called artificial neurons or nodes) connected to each other by weighting. The weights on each connection can be dynamically adjusted until the desired output is generated for a given input. An artificial neuron model consists of a linear combination followed by an activation function. Different types of activation functions can be utilized for the network; nevertheless, the common ones, which are sufficient for most applications, are the sigmoid and hyperbolic tangent functions [10].

In the input and hidden layers, neural networks contain neurons with nonlinear activation functions, whereas in the output layer, neural networks contain neurons with linear activation functions. ANN has multi-layer perceptron (MLP) structure, which uses forward propagation neural network. Various training algorithms exist for MLP. In this work, we used the Scaled Conjugate Gradient Backpropagation (SCG) algorithm which is based on the conjugate directions. Block diagram of the proposed ANN based technique is shown in Figure 2.

The estimator uses the information provided by the reference symbols to estimate the total channel frequency response. At the beginning of the estimation process, the complex signal is split into two parts: real and imaginary. These parts are normalized between -1 and +1 before training.

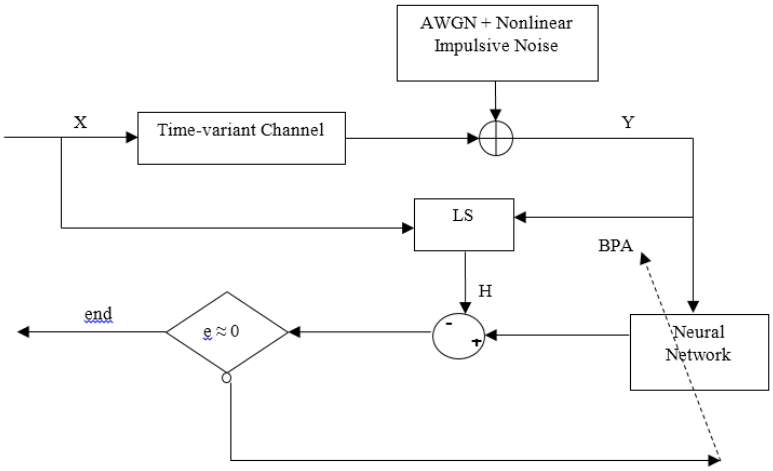

Figure 2: ANN channel estimation trained by Back-Propagation Algorithm.

The adopted architecture of neural network is chosen after multiple tests of convergence by minimizing the learning time and keeping low implementation complexity.

The output of a single neuron is given by the following equation:

$$\hat{A}_j = f\left(\sum_{i=0}^{2N_P-1} w_{j,i}\, P_i + b_j\right) \tag{6}$$

where, $\hat{A}_j$ is the neuron output in the range of $(0 \le j \le 2N-1)$ since there are N real part and N imaginary part of $\hat{A}_j$, $w_{j,i}$ is a value of the synaptic weight connecting the stimulus i to the neuron j, P_i, is the input stimulus, b_j is the bias of neuron j, and f is the neuron output sigmoid function. The weights $w_{j,i}$ are updated with the SCG backpropagation algorithm.

The estimator training operation consists of changing the values of interconnection weights using learning algorithms for obtaining the desired performance. The learning algorithm in our neural network is the efficient gradient back propagation based on the minimization of the average square error (for all $2N$ output neurons) expressed as

$$e = \frac{1}{N_l}\sum_{l=0}^{N_l-1}\sum_{j=0}^{2N-1}\left(e_j^l\right)^2 \tag{7}$$

where e_j^l represents the error on the j^{th} neuron output from the l^{th} example of training set.

After completing the training phase, the network uses the input data from the pilot channels to estimate all the data channels. Subsequently, the equalization is followed by a decision estimate of the OFDMA symbols. For a single training operation, the neural network estimates a large number of OFDM symbols corresponding to several radio frames LTE.

4 Complex SVR estimation

First, let the OFDM frame contains Ns OFDM symbols which every symbol includes N subcarriers. Then, we exploit the index of the pilots in the OFDM symbols in order to estimate the channel frequency

responses at these positions. The transmitting pilot symbols are $\boldsymbol{X}^P = diag(X\ (i, m\,\Delta P)), m = 0,1,\cdots, N_P - 1$, where i and m are labels in time domain and frequency domain respectively, and ΔP is the pilot interval in frequency domain.

The proposed channel estimation method is based on complex SVR algorithm which has two separate phases: learning phase and estimation phase. In training phase, we estimate first the subchannels pilot symbols according to LS criterion to strike $min\ [(Y^P - \boldsymbol{X}^P \boldsymbol{F} h)\ (Y^P - \boldsymbol{X}^P \boldsymbol{F} h)^H]$ [11], as

$$\widehat{H}^P = \boldsymbol{X}^{P\ -1}\ Y^P \tag{8}$$

where $Y^P = Y\ (i, m\,\Delta P)$ and $\widehat{H}^P = \widehat{H}\ (i, m\,\Delta P)$ are the received pilot symbols and the estimated frequency responses for the i^{th} OFDM symbol at pilot positions $m\ \Delta P$, respectively.

Then, in the estimation phase and by the interpolation mechanism, frequency responses of data subchannels will be predicted based on the regression model built in training space. Therefore, frequency responses of all the OFDM subcarriers are

$$\widehat{H}\ (i, q\ ) = f\left(\widehat{H}^P (i, m\,\Delta P)\right) \tag{9}$$

where $q = 0, \cdots, N - 1$, and $f(\cdot)$ is the interpolating function, which is determined by the nonlinear complex SVR approach.

In fact, in a nonlinear deep fading channel, it is necessary to apply the nonlinear complex SVR technique for channel estimation since SVM is superior in solving nonlinear, small samples and high dimensional pattern recognition [12]. The basic idea of Mercer's theorem is that a vector in the input space (finite dimensional space) can be mapped to a higher dimensional feature space $\mathcal{H}$ (possibly infinity) by means of nonlinear transformation $\boldsymbol{\varphi}$. However, this transformation usually remains unknown. Hence, only the dot product of the corresponding space is required and can be stated as a function of the input vectors as following:

$$\boldsymbol{K}(\boldsymbol{x}_i, \boldsymbol{x}_j) = \langle \boldsymbol{\varphi}(\boldsymbol{x}_i), \boldsymbol{\varphi}(\boldsymbol{x}_j) \rangle \tag{10}$$

Such spaces are known as Reproducing Kernel Hilbert Spaces (RKHS) where $\boldsymbol{K}(\boldsymbol{x}_i, \boldsymbol{x}_j)$ is the kernel that satisfy the conditions of Mercer's theorem (it is the inner product of a Hilbert space). In this paper, we are using the Radial Basis Function (RBF) which is expressed as

$$\boldsymbol{K}(\boldsymbol{x}_i, \boldsymbol{x}_j) = \exp\left(-\frac{\|\boldsymbol{x}_i - \boldsymbol{x}_j\|^2}{2\sigma^2}\right) \tag{11}$$

After mapping the input vectors to a higher-dimensional feature space using the nonlinear transformation $\boldsymbol{\varphi}$, the linear regression function can be stated as follows:

$$\widehat{H}(m\,\Delta P) = \boldsymbol{w}^{\boldsymbol{T}} \boldsymbol{\varphi}(m\,\Delta P) + b + e_m, \qquad m = 0, \cdots, N_P - 1 \tag{12}$$

where $\boldsymbol{w}$ is the weight vector, b is the bias term well known in the SVM literature and residuals $\{e_m\}$ account for the effect of both approximation errors and noise. In the SVM framework, the optimality criterion is a regularized and constrained version of the regularized Least Squares criterion.

In general, SVM algorithms minimize a regularized cost function of the residuals, usually the Vapnik's $\varepsilon - insensitivity$ cost function [8].

A robust cost function is introduced to improve the performance of the estimation algorithm which is ε -Huber robust cost function [11] [13], given by

$$\mathcal{L}^{\varepsilon}(e_m) = \begin{cases} 0, & |e_m| \le \varepsilon \\ \frac{1}{2\gamma}(|e_m| - \varepsilon)^2, & \varepsilon \le |e_m| \le e_C \\ C(|e_m| - \varepsilon) - \frac{1}{2}\gamma C^2, & e_C \le |e_m| \end{cases} \tag{13}$$

where $e_C = \varepsilon + \gamma C$, ε is the insensitive parameter which is positive scalar that represents the insensitivity to a low noise level, parameters γ and C control essentially the trade-off between the regularization and the losses, and represent the relevance of the residuals that are in the linear or in the quadratic cost zone, respectively. The cost function is linear for errors above e_C, and quadratic for errors between ε and e_C. Note that, errors lower than ε are ignored in the $\varepsilon - insensitivite$ zone. On the other hand, the quadratic cost zone uses the $L_2 - norm$ of errors, which is appropriate for Gaussian noise, and the linear cost zone limits the effect of sub-Gaussian noise [14]. Therefore, the ε -Huber robust cost function can be adapted to different types of noise.

Let us assume that $\mathcal{L}^{\varepsilon}(e_m) = \mathcal{L}^{\varepsilon}\big(\mathcal{R}(e_m)\big) + \mathcal{L}^{\varepsilon}\big(\Im(e_m)\big)$ since $\{e_m\}$ are complex, where $\mathcal{R}(\cdot)$ and $\Im(\cdot)$ represent real and imaginary parts, respectively. Now, the SVR primal problem can be stated as minimizing

$$\frac{1}{2}\|\boldsymbol{w}\|^2 + \frac{1}{2\gamma}\sum_{m\in I_1}(\xi_m + \xi_m^*)^2 + C\sum_{m\in I_2}(\xi_m + \xi_m^*) + \frac{1}{2\gamma}\sum_{m\in I_3}(\zeta_m + \zeta_m^*)^2 + C\sum_{m\in I_4}(\zeta_m + \zeta_m^*) - \frac{1}{2}\sum_{m\in I_2, I_4}\gamma C^2 \tag{14}$$

constrained to

$$\begin{aligned} \mathcal{R}\big(\widehat{H}(m\,\Delta P) - \boldsymbol{w^T}\boldsymbol{\varphi}(m\,\Delta P) - b\big) &\le \varepsilon + \xi_m \\ \Im\big(\widehat{H}(m\,\Delta P) - \boldsymbol{w^T}\boldsymbol{\varphi}(m\,\Delta P) - b\big) &\le \varepsilon + \zeta_m \\ \mathcal{R}(-\widehat{H}(m\,\Delta P) + \boldsymbol{w^T}\boldsymbol{\varphi}(m\,\Delta P) + b) &\le \varepsilon + \xi_m^* \\ \Im(-\widehat{H}(m\,\Delta P) + \boldsymbol{w^T}\boldsymbol{\varphi}(m\,\Delta P) + b) &\le \varepsilon + \zeta_m^* \\ \xi_m^{(*)}, \zeta_m^{(*)} &\ge 0 \end{aligned} \tag{15}$$

for $m = 0, \cdots, N_P - 1$, where ξ_m and ξ_m^* are slack variables which stand for positive and negative errors in the real part, respectively. ζ_m and ζ_m^* are the errors for the imaginary parts. I_1, I_2, I_3 and I_4 are the set of samples for which:

I_1 : real part of the residuals are in the quadratic zone;

I_2 : real part of the residuals are in the linear zone;

I_3 : imaginary part of the residuals are in the quadratic zone;

I_4 : imaginary part of the residuals are in the linear zone.

To transform the minimization of the primal functional (14) subject to constraints in (15), into the optimization of the dual functional, we must first introduce the constraints into the primal functional by means of Lagrange multipliers to obtain the primal-dual functional. Then, by making zero the primal-dual functional gradient with respect to ϖ_i, we obtain an optimal solution for the weights

$$\boldsymbol{w} = \sum_{m=0}^{N_P-1} \psi_m \, \boldsymbol{\varphi}(m\,\Delta P) = \sum_{m=0}^{N_P-1} \psi_m \, \boldsymbol{\varphi}(P_m) \tag{16}$$

where $\psi_m = (\alpha_{\mathcal{R},m} - \alpha^*_{\mathcal{R},m}) + j(\alpha_{I,m} - \alpha^*_{I,m})$ with $\alpha_{\mathcal{R},m}, \alpha^*_{\mathcal{R},m}, \alpha_{I,m}, \alpha^*_{I,m}$ are the Lagrange multipliers (or dual variables) for real and imaginary part of the residuals and $P_m = (m\,\Delta P)$, $m = 0, \cdots, N_P - 1$ are the pilot positions.

In order to solve the dual function, we define the Gram matrix as

$$\boldsymbol{G}(u,v) =< \boldsymbol{\varphi}(P_u), \boldsymbol{\varphi}(P_v) >= K(P_u, P_v) \tag{17}$$

where $K(P_u, P_v)$ is a Mercer's kernel which represents the RBF kernel matrix which allows obviating the explicit knowledge of the nonlinear mapping $\boldsymbol{\varphi}(\cdot)$. A simplified compact form of the functional problem can be stated in matrix format by placing optimal solution $\boldsymbol{w}$ into the primal dual functional and grouping terms. Subsequently, the dual problem consists of maximizing

$$max \; -\frac{1}{2}\boldsymbol{\psi}^H(\boldsymbol{G} + \gamma \boldsymbol{I})\boldsymbol{\psi} + \mathcal{R}\left(\boldsymbol{\psi}^{\boldsymbol{H}} Y^P\right) - (\boldsymbol{\alpha}_{\boldsymbol{\mathcal{R}}} + \boldsymbol{\alpha}^*_{\boldsymbol{\mathcal{R}}} + \boldsymbol{\alpha}_{\boldsymbol{I}} + \boldsymbol{\alpha}^*_{\boldsymbol{I}})\mathbf{1}\mathcal{E} \tag{18}$$

constrained to

$$0 \leq \alpha_{\mathcal{R},m}, \alpha^*_{\mathcal{R},m}, \alpha_{I,m}\,, \alpha^*_{I,m} \leq C \tag{19}$$

where $\boldsymbol{\psi} = [\psi_0, \cdots, \psi_{N_P-1}]^T$; **I** and **1** are the identity matrix and the all-ones column vector, respectively; $\boldsymbol{\alpha}_{\boldsymbol{\mathcal{R}}}$ is the vector which contains the corresponding dual variables, with the other subsets being similarly represented. The weight vector can be obtained by optimizing (18) with respect to $\alpha_{\mathcal{R},m}, \alpha^*_{\mathcal{R},m}, \alpha_{I,m}\,, \alpha^*_{I,m}$ and then substituting into (16).

Therefore, and after training phase, frequency responses at all subcarriers in each OFDM symbol can be obtained by SVR interpolation

$$\widehat{H}(k) = \sum_{m=0}^{N_P-1} \psi_m \, K(P_m, k) + b \tag{20}$$

for $k = 1, \cdots, N$. Note that, the obtained subset of Lagrange multipliers which are nonzero will provide with a sparse solution (and they represent the support vectors). Equation (20) will be used in the estimation step to predict the channel for the data symbols. As usual in the context of SVM framework, the free parameters of the kernel and the cost function represent limited freedom for the user and have to be fixed manually after gaining some a priori knowledge of the problem, or by using some validation set of observations [8].

5 Simulation results

In this part of our analysis, we compare the proposed algorithms (ANN with Backpropagation SCG algorithm and nonlinear complex RBF-based SVR algorithm) with the LS, Decision Feedback and perfect estimation based on Bit Error Rate (BER) and Mean Square Error (MSE) curves. We will analyze the

performance of our algorithms in terms of robustness against fading joint with nonlinear noise, and complexity.

We consider the channel impulse response of the time varying multipath fading channel model which can be written as

$$h(\tau,t)=\sum_{l=0}^{L-1}h_l(t)\,\delta(t-\tau_l) \tag{21}$$

where $h_l(t)$ is the impulse response representing the complex attenuation of the l^{th} path, τ_l is the random delay of the l^{th} path and L is the number of multipath replicas. The specification parameters of an extended vehicular A model (EVA) for LTE DL system with the excess tap delay and the relative power for each path of the channel are shown in table 1. These parameters are defined by 3GPP standard [15].

Table 1. Extended Vehicular A model (EVA) [15].

Excess tap delay [ns]	Relative power [dB]
0	0.0
30	-1.5
150	-1.4
310	-3.6
370	-0.6
710	-9.1
1090	-7.0
1730	-12.0
2510	-16.9

Figure 3 presents the variations in time and in frequency of the channel frequency response for a mobile speed equal to 350 Km/h.

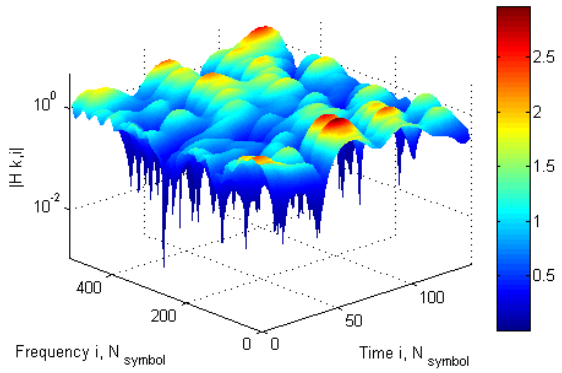

Figure 3: Variation in time and in frequency for a mobile speed at 350 Km/h.

In order to demonstrate the effectiveness of the presented techniques and evaluate the performance in the presence of nonlinear impulsive noise under high mobility conditions (350Km/h), two objective criteria are used: the signal-to-noise ratio (SNR) and signal-to-impulse ratio (SIR).

The expressions of SNR and SIR are given by [8]

$$SNR_{dB} = 10log_{10}\left(\frac{E\{|y(n) - w(n) - i(n)|^2\}}{\sigma_w^2}\right) \quad (22)$$

and

$$SIR_{dB} = 10log_{10}\left(\frac{E\{|y(n) - w(n) - i(n)|^2\}}{\sigma_{BG}^2}\right) \quad (23)$$

Then, we simulate the OFDM LTE DL system with parameters presented in Table 2. The proposed algorithms estimate a number of OFDM symbols in the range of 1400 symbols, corresponding to 10 radio frames LTE. Note that, the LTE radio frame duration is 10 ms [16], which is divided into 10 subframes. Each subframe is further divided into two slots, each of 0.5ms duration, as presented in Figure 4.

Table 3. Parameters of simulations [16], [17] and [18].

Parameters	Specifications
OFDM system	LTE/Downlink
Constellation	16-QAM
Mobile Speed (Km/h)	350
T_s (µs)	72
f_c (GHz)	2.15
δf (KHz)	15
B (MHz)	5
Size of DFT/IDFT	512
Number of paths	9

The variation of BER and MSE as a function of SNR in the presence of AWGN noise for a mobile speed at 350 Km/h is shown in Figs. 5 (a) and (b). The complex RBF-based SVR method slightly outperforms ANN with Backpropagation SCG algorithm and noticeably outperforms LS and DF methods. For example, we can see a gain of 10 dB over the DF method. We can also see that the SVR and ANN performances are close to the perfect channel knowledge estimation compared to others estimation techniques. These results demonstrate the advantage of the nonlinear complex SVR and its ability to adapt to the channel variations, providing a better channel estimation which gives an improvement of the service quality in LTE DL. MSE confirms the results obtained for BER and shows that LS suffers from a high MSE, however, complex SVR and ANN have low MSE.

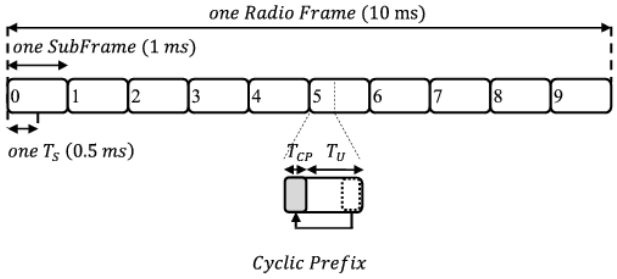

Figure 4: LTE frame structure

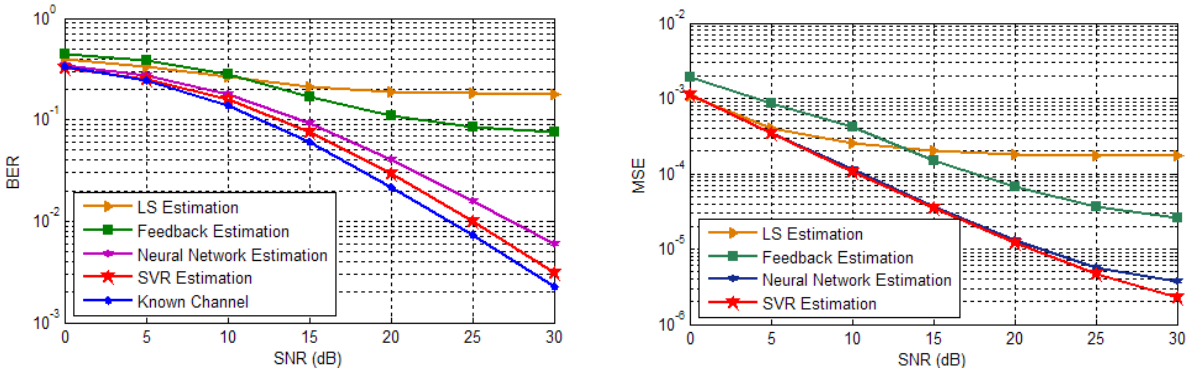

Figure 5: (a) BER and (b) MSE vs. SNR for a mobile speed at 350 Km/h without impulsive noise.

Figs. 6 (a) and (b) show the performance of LS, DF, ANN and complex SVR estimation techniques in the presence of AWGN noise and nonlinear impulsive noise with *SIR* = -5dB and *p* = .05 for a mobile speed at 350 Km/h. A poor performance is exhibited by LS and DF for all noise levels and good performance is observed with complex SVR which still track the estimation with perfect channel and also outperforms ANN. The MSE performance among these techniques ranges from best to the worst as follows: complex RBF-SVR based technique; SCG-ANN based technique, DF and LS.

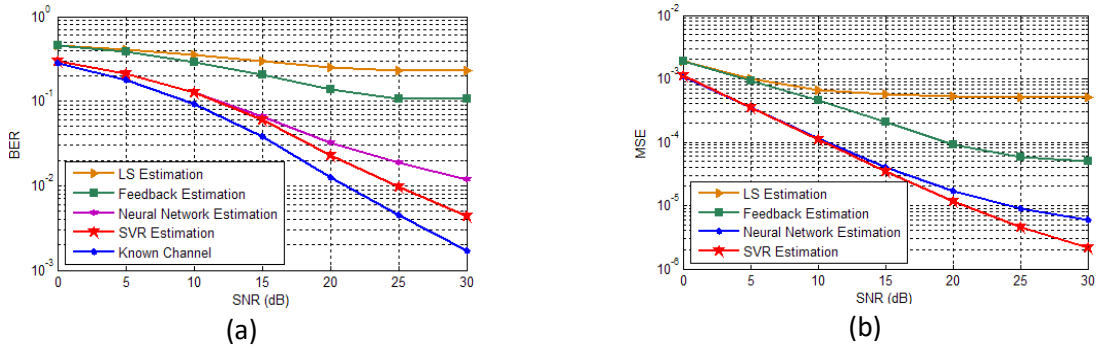

Figure 6: (a) BER and (b) MSE vs. SNR for a mobile speed at 350 Km/h with SIR = -5 dB and p = .05.

Figs. 7 (a) and (b) show the BER and MSE performances of LS, DF, ANN and complex SVR techniques in the presence of non-Gaussian impulsive noise with *p* = .05 for *SNR* = 30 dB as a function of SIR which is ranged from -20 to 20 dB. These figures confirm that nonlinear complex SVR algorithm performs better than LS, DF and also ANN algorithms in high-mobility environments presenting high levels of impulsive noise (SIR<0 dB), which proves that the RBF-SVR based approach is powerful in the nonlinear environments.

6 Conclusion

In this paper, we analyzed the performance of the scaled conjugate gradient backpropagation ANN and the complex RBF-based SVR algorithms for the channel estimation in the LTE DL system. These methods are based on two steps: the learning step where each method tries to adapt to the channel variations and constructs the regression model and the estimation step where the channel frequency response will be estimated.

The proposed methods where applied to vehicular A channel model according to 3GPP specifications in the presence of nonlinear impulsive noise interfering with OFDM pilot symbols in high-mobility environment. The simulation results clearly show that the nonlinear complex RBF-based SVR method

produces a good performance when compared to LS, Decision Feedback and ANN. The obtained results are very promising for improving the service quality in the LTE DL system. We still work on adopting this technique as channel estimator in LTE-Advanced systems.

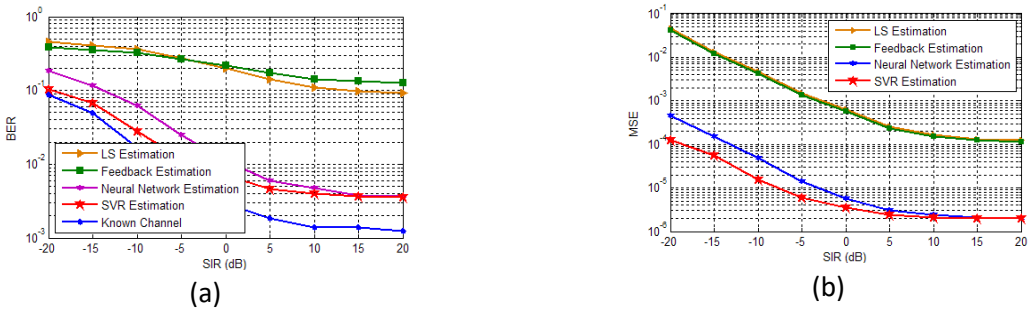

(a) (b)

Figure 7: (a) BER and (b) MSE vs. SIR for a mobile speed at 350 Km/h with SNR = 30 dB and p = .05.

REFERENCES

[1]. Dahlman, E., S. Parkvall, J. Skold and P. Berning, *3G Evolution-HSPA and LTE for mobile broadband*. 2nd edition 2008, New York: vol. Academic.

[2]. Colieri, S., M. Ergen, A. Puri and A. Bahai. *A study of channel estimation in OFDM systems*. In Proceedings of the IEEE 56th Vehicular Technology Conference, 2002, vol. 2: p. 894–898.

[3]. Colieri, S., M. Ergen, A. Puri and A. Bahai. *Channel estimation techniques based on pilot arrangement in OFDM systems*. IEEE Transactions on Broadcasting, 2002, vol. 48, no. 3: p. 223–229.

[4]. Patra, J. C., R. N. Pal, R. Baliarsingh and G. Panda. *Nonlinear channel equalization for QAM signal constellation using artificial neural networks*. IEEE Transactions on Systems, Man, and Cybernetics, 1999, vol. 29, no. 2, p. 254–262.

[5]. Naveed, A., I. M. Qureshi, T. A. Cheema, and A. Jalil. *Blind equalization and estimation of channel using artificial neural network*, 8th International Multitopic Conference, INMIC, 2004, p. 184–190.

[6]. Fernández-Getino García, M. J., J. M. Páez-Borrallo, and S. Zazo. *DFT-based channel estimation in 2D-pilot-symbol-aided OFDM wireless systems*. IEEE Vehicular Technology Conf., 2001, vol. 2, p. 815–819.

[7]. Sliskovic, M. *Signal processing algorithm for OFDM channel with impulse noise*. IEEE conf. on Electronics, Circuits and Systems, 2000, p. 222–225.

[8]. Rojo-Álvarez, J. L., C. Figuera-Pozuelo, C. E. Martínez-Cruz, G. Camps-Valls, F. Alonso-Atienza, M. Martínez-Ramón. *Nonuniform interpolation of noisy signals using support vector machines*. IEEE Trans. Signal process., 2007, vol. 55, no.48, p. 4116–4126.

[9]. Nanping, L., Y. Yuan, X. Kewen, and Z. Zhiwei. *Study on channel estimation technology in OFDM system*. IEEE Computer Society Conf., 2009, p. 773–776.

[10]. Çiikli, C., A. T. Özsahin, A. C. Yapici. *Artificial neural network channel estimation based on Levenberg-Marquardt for OFDM systems*. Wireless Pers. Commun., 2009, p. 221–229.

[11]. Charrada, A and A. Samet. *Estimation of highly selective channels for OFDM system by complex least squares support vector machines. Int. J. Electron. Commun. (AEÜ), 2012, vol. 66, p. 687-692.*

[12]. Nanping, L., Y. Yuan, X. Kewen and Z. Zhiwei. *Study on channel estimation technology in OFDM system*. IEEE Computer Society Conf., 2009, p. 773–776.

[13]. Charrada, A and A. Samet. *Nonlinear Complex LS-SVM for Highly Selective OFDM Channel with Impulse Noise. 6th International Conference on Sciences of Electronics, Technologies of Information and Telecommunications (SETIT), 2012, p. 696-700.*

[14]. Fernández-Getino García, M. J., J. L. Rojo-Álvarez, F. Alonso-Atienza, and M. Martínez-Ramón. *Support vector machines for robust channel estimation in OFDM*. IEEE signal process. J., 2006, vol. 13, no. 7.

[15]. 3rd Generation Partnership Project. Technical Specification Group Radio Access Network: evolved Universal Terrestrial Radio Access (UTRA): Base Station (BS) radio transmission and reception. *TS 36.104*, September 2009, V8.7.0.

[16]. 3rd Generation Partnership Project. Technical Specification Group Radio Access Network: evolved Universal Terrestrial Radio Access (UTRA): Physical Channels and Modulation layer. *TS 36.211*, September 2009, V8.8.0.

[17]. 3rd Generation Partnership Project. Technical Specification Group Radio Access Network: Physical layer aspects for evolved Universal Terrestrial Radio Access (UTRA). *TR 25.814*, September 2006, V7.1.0.

[18]. 3rd Generation Partnership Project. Technical Specification Group Radio Access Network: evolved Universal Terrestrial Radio Access (UTRA): Physical layer procedures. *TS 36.213*, September 2009, V8.8.0,